

Valence bond glass — A unified theory of electronic disorder and pseudogap phenomena in high temperature superconductors

Liang Ren and Ziqiang Wang

Department of Physics, Boston College, Chestnut Hill, Massachusetts 02467

We show that the low-energy fluctuations of the valence bond in underdoped high- T_c cuprates, originating from quantum fluctuations of the superexchange interaction, are pinned by the electronic disorder due to off-stoichiometric dopants, leading to a valence bond glass (VBG) pseudogap phase. The antinodal Fermi surface sections are gapped out, giving rise to a normal state Fermi arc whose length shrinks with underdoping below a temperature T^* determined by thermal filling. Below T_c , the superexchange interaction induces a d -wave superconducting gap that coexists with the VBG pseudogap. The evolution of the local and momentum-space spectroscopy with doping and temperature captures the salient properties of the pseudogap phenomena and the electronic disorder revealed by recent ARPES and STM experiments. Our unified theory elucidates the interplay between strong correlation and the intrinsic electronic disorder in doped transition metal oxides.

The most unconventional electronic state in the high- T_c cuprates lies in the pseudogap phase that straddles the AF Mott insulator and the d -wave superconductor. The origin of the pseudogap phase is a subject of intensive debate in connection to the emergent quantum electronic matter in doped Mott insulators [1]. This unexpected phase is defined by the emergence of a normal state *pseudogap* in the single-particle excitation spectrum below a characteristic temperature T^* [2, 3]. One of the most intriguing properties is the pseudogap anisotropy in momentum space: the Fermi surface (FS) near the d -wave antinodes is gapped out, leaving a Fermi arc of gapless excitations near the nodes. This nodal-antinodal dichotomy is further enlightened by recent ARPES [4, 5, 6] and Raman [7] experiments that find two distinct pieces in the spectral gap in terms of temperature and doping dependence: a large pseudogap near the antinodes that tracks T^* and a smaller superconducting (SC) gap that opens along the arc that tracks T_c . Recent STM measurements find a less disordered SC gap coexisting with a large inhomogeneous pseudogap below T_c in the local density of states (DOS) [8, 9].

The Fermi arc raises the possibility for an unconventional electronic state. In the absence of disorder, the FS is the trajectory of the poles in the single-particle Green's function and involves continuous contours in momentum space. Thus the Fermi arc must evolve into either a Fermi point or a FS pocket at low temperatures. This difference highlights two kinds of proposals for the origin of the pseudogap: the one-gap and two-gap scenarios. The one-gap scenario attributes the pseudogap to a d -wave pairing gap without SC phase coherence that evolves into a single d -wave SC gap below T_c [1, 10, 11]. The two-gap scenario accounts for the pseudogap as due to competing order from an energetically favorable state unrelated to pairing. An important implication of a generic two-gap scenario is the *coexistence* of a d -wave SC gap over the Fermi arc and a low-temperature pseudogap in the antinodal region below T_c [12]. The observation of two distinct gaps by ARPES, Raman, and STM experiments discussed above provides strong support for the two-gap scenario.

A consistent theory for the pseudogap has been challenging. Most of the proposals for a competing state invoke various

density waves and flux/orbital current order [1, 10] that break translation symmetry by one lattice constant and result in superstructures. The FS is removed from the antinodal region by folding the band with respect to a unique ordering wavevector q which generically leads to FS pockets. However, despite many years of effort and the much improved measurement resolution, no signatures of disguised FS pockets or folded bands have been detected. Moreover, the pseudogap produced by these density wave orders is generically particle-hole asymmetric [13], which is inconsistent with the V-shaped averaged DOS at low energies observed in tunneling experiments.

A related phenomenon in the cuprates is the electronic disorder. There has been mounting STM evidence for nanoscale DOS gap disorder [14, 15, 16, 17, 18] and, under a variety of conditions where superconductivity is weakened, short-range ordered checkerboard DOS modulations [15, 18, 19, 20] which are manifestations of a bond-centered electronic glass [21]. A natural cause for the electronic disorder is the out of plane ionic dopants, interstitial in $\text{Bi}_2\text{Sr}_2\text{CaCu}_2\text{O}_{8+x}$, substitutional in $\text{La}_{2-x}\text{Sr}_x\text{CuO}_4$ and $\text{Ca}_{2-x}\text{Na}_x\text{CuO}_2\text{Cl}_2$, and in combination with chemical substitutions in $\text{Bi}_2\text{Ln}_{2-z}\text{Bi}_z\text{CuO}_{6+x}$ (Ln-Bi2201). In addition to inducing structural distortions, the screening of the dopant electrostatic potential is highly nonlinear in doped Mott insulators due to strong Coulomb repulsion, leading to inhomogeneous electronic states with spatial variations in the local doping concentration [22, 23].

We present here a unified theory for the pseudogap phenomena and the electronic disorder. The key point is the interplay between strong correlation induced valence bond fluctuations and the dopant induced disorder. In the parent compounds, the superexchange interaction between the Cu spins, described by the nearest neighbor Heisenberg model $H_J = J \sum_{\langle i,j \rangle} \mathbf{S}_i \cdot \mathbf{S}_j$, causes antiferromagnetic (AF) order in the ground state. Due to strong quantum fluctuations of the spin-1/2 moment, the nonmagnetic *valence bond states* are close in energy to the AF state. Writing $\mathbf{S}_i \cdot \mathbf{S}_j = \frac{1}{2} c_{i\sigma}^\dagger c_{i\sigma'} c_{j\sigma'}^\dagger c_{j\sigma} + \text{const.}$, the valence bond can be formed via either spin-singlet pairing $\Delta_{ij} = \langle c_{i\uparrow} c_{j\downarrow} - c_{i\downarrow} c_{j\uparrow} \rangle$ or the paramagnetic valence bond $\chi_{ij} = \langle c_{i\sigma}^\dagger c_{j\sigma} \rangle$, as envisioned by Pauling in chemical

bonding and revived by Anderson in the resonance valence bond (RVB) theory [24]. Since charge fluctuations are completely suppressed, the two descriptions are equivalent at half-filling. Owing to an SU(2) symmetry [25], the valence bond states are highly degenerate. Besides translation invariant valence bond liquid states, there are also symmetry breaking valence bond crystal states which are gapped but competitive in energy [1, 26]. Doping the Mott insulator breaks the SU(2) symmetry and makes the valence bond in the particle-particle and particle-hole channels different. The basic question is which fluctuating valence bond state is selected when a sufficient amount of holes destroys the AF long-range order. In the short-range RVB theory, the spin-singlet pairs are mobilized by the doped holes and condense into a d-wave SC state [27]. There is, however, a natural competing order driven by the same superexchange interaction J that is associated with the valence bond χ_{ij} in the particle-hole channel [13].

We show that the d -wave component of the *real part* of χ_{ij} represents the most important low-energy fluctuations and that dopant induced electron disorder pins such d -wave charge density wave fluctuations to form an electronic valence bond glass (VBG) phase exhibiting the observed pseudogap phenomena. This is similar in spirit to the disorder induced glassy phases or the nematic liquid crystal of stripes [28]. A ubiquitous feature of the VBG is the emergence of a pseudogap near the antinodes where the valence bond fluctuations are large due to the flatness of the band, giving rise to a genuine normal state Fermi arc. Based on microscopic calculations of the extended t-J model using spatially unrestricted Gutzwiller approximation, we show that the VBG captures the salient properties of the pseudogap phenomena and electronic disorder observed in recent ARPES and STM experiments, especially in underdoped and chemically substituted bilayer and single-layer Bi-based cuprates where the pseudogap and the SC gap scales are well separated [4, 5, 6, 8, 9].

The Hamiltonian of the extended t-J model is given by

$$H = - \sum_{i \neq j} t_{ij} P_i c_{i\sigma}^\dagger c_{j\sigma} P_j + J \sum_{\langle i,j \rangle} (\mathbf{S}_i \cdot \mathbf{S}_j - \frac{1}{4} \hat{n}_i \hat{n}_j) + \sum_i V_i \hat{n}_i. \quad (1)$$

The electrons hop between near neighbors via t_{ij} . Repeated spin indices are summed, $\hat{n}_i = c_{i\sigma}^\dagger c_{i\sigma}$, $\mathbf{S}_i = \frac{1}{2} c_{i\sigma}^\dagger \boldsymbol{\tau}_{\sigma\sigma'} c_{i\sigma'}$. The local doping is given by $x_i = 1 - n_i$ with $n_i = \langle c_{i\sigma}^\dagger c_{i\sigma} \rangle$. The projection operator P_i removes double occupation on site- i . The last term in Eq. (1) is the electrostatic potential, $V(i) = \sum_{j \neq i} \frac{V_c}{|r_i - r_j|} (n_j - \bar{n}) + \sum_{\ell=1}^{N_d} \frac{V_d}{\sqrt{|r_i - r_\ell|^2 + d_s^2}}$, where the long-range Coulomb interaction of strength V_c between the in-plane electrons provides the important screening of the ionic potential of strength V_d due to N_d number of off-plane dopants with a set back distance d_s [22, 23]. We use $J = 120\text{meV}$ and the near neighbor hopping $t = (360, -120, 29, 24, -24)\text{meV}$ relevant for the cuprate band structure [29] and set $V_c = V_d = 0.5\text{eV}$ and $d_s = 1$ in units of the lattice constant. To account for the Coulomb repulsion between the ionized dopants, the dopant configurations are generated randomly with a hard-core of one to three lattice spacings.

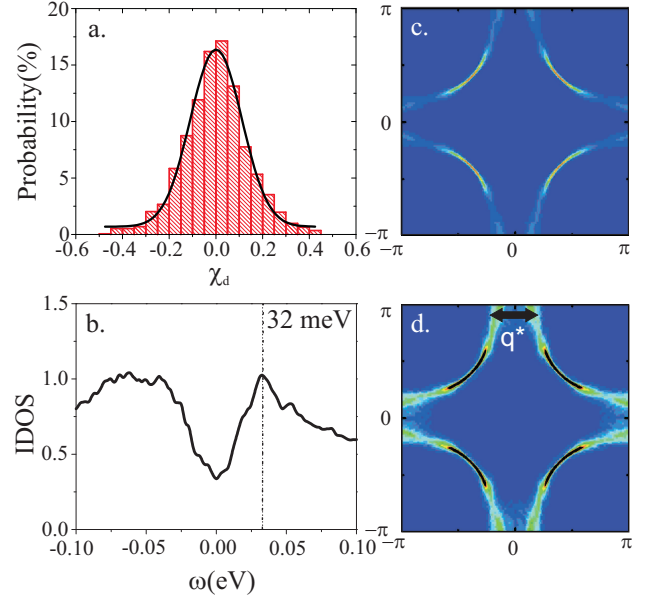


Figure 1: Normal state pseudogap and Fermi arc at $x = 0.125$. (a) Distribution of d -wave valence bond showing glassy order. (b) Averaged DOS showing VBG pseudogap. (c) and (d) Fermi arc.

To account for both strong correlation and disorder, we use the spatially unrestricted Gutzwiller projected wave function $|\Psi\rangle = \prod_i y_i^{\hat{n}_i} (1 - \hat{n}_{i\uparrow} \hat{n}_{i\downarrow}) |\Psi_0\rangle$, where Ψ_0 is a Slater determinant state and y_i is a *local* fugacity that keeps the density unchanged before and after projection. The projection is implemented using the Gutzwiller approximation [30, 31], where the t-J Hamiltonian in the projected Hilbert space is replaced by one in the unprojected space with renormalized hopping and exchange that captures the basic Mott physics: $t_{ij} \rightarrow g_{ij}^t t_{ij}$ and $J \rightarrow g_{ij}^J J$. In a disordered state, $g_{ij}^t = \sqrt{4x_i x_j / (1 + x_i)(1 + x_j)}$, $g_{ij}^J = 4 / (1 + x_i)(1 + x_j)$ depend on the *local doping* [13]. Decoupling the exchange interaction in terms of the valence bond χ_{ij} and singlet pairing Δ_{ij} , we obtain a Gutzwiller renormalized Hamiltonian,

$$H_{GA} = - \sum_{i \neq j} g_{ij}^t t_{ij} c_{i\sigma}^\dagger c_{j\sigma} + \sum_i (V_i + \lambda_i) c_{i\sigma}^\dagger c_{i\sigma} - \sum_i \lambda_i n_i - \frac{1}{4} J \sum_{\langle i,j \rangle} g_{ij}^J \left(\chi_{ij}^* c_{i\sigma}^\dagger c_{j\sigma} + \text{h.c.} - |\chi_{ij}|^2 \right) - \frac{1}{4} J \sum_{\langle i,j \rangle} g_{ij}^\Delta \left(\Delta_{ij}^* \epsilon_{\sigma\sigma'} c_{i\sigma} c_{j\sigma'} + \text{h.c.} - |\Delta_{ij}|^2 \right), \quad (2)$$

where $g_{ij}^J = g_{ij}^\Delta = g_{ij}^J$ and λ_i originates from the local fugacity. We minimize the ground state energy of Eq. (2) through self-consistently determined $\{x_i, \lambda_i, \chi_{ij}, \Delta_{ij}\}$ on 24×24 systems for different dopant configurations.

Normal state VBG pseudogap phase. In the normal state above T_c or the zero temperature phase with $\Delta_{ij} = 0$, we find that the valence bond χ_{ij} is *real* and fluctuates due to the disorder potential in the doping range studied. The dominant fluctuation is in the d -wave channel, $\chi_d(i) = \frac{1}{4} \sum_j d_{ij} \chi_{ij}$, with the form factor $d_{ij} = \pm 1$ for the four bonds emanating from

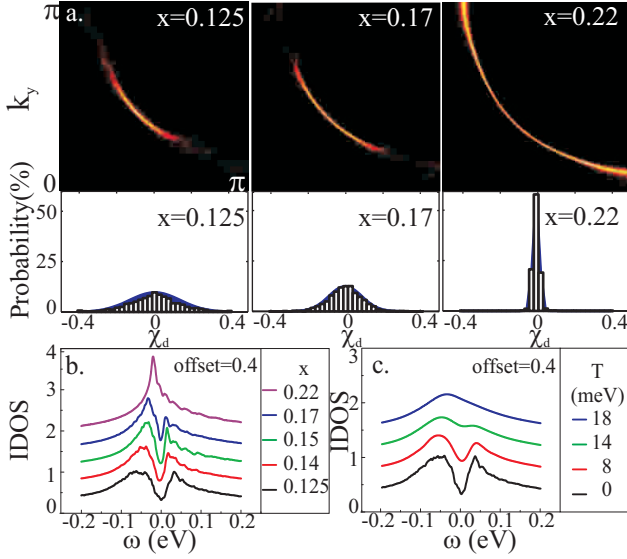


Figure 2: Doping dependence of the Fermi arc and valence bond glassy order (a) and averaged DOS and pseudogap (b). (c) Temperature evolution of VBG pseudogap at $x = 0.125$.

site i . The histogram of χ_d at average doping $x = 0.125$ is shown in Fig. 1a. It follows a Gaussian distribution with zero mean. The root-mean-squared fluctuation represents a nonzero “glassy” order parameter $\delta_\chi = \sqrt{\sum_i \chi_d^2(i)/N_s} = 0.28$ for the VBG phase. The most succinct feature of the VBG is the emergence of the pseudogap and the Fermi arc. The integrated DOS (IDOS) in Fig. 1b shows a remarkable V-shaped pseudogap, $\Delta_{pg} \sim 32\text{meV}$, approximately symmetrically distributed around the Fermi level due to the d -wave VBG order. The calculated spectral intensity at the Fermi energy shown in Fig. 1c reveals a FS truncated near the antinodes by the pseudogap and a Fermi arc around the nodes. The Fermi arc tracks the underlying FS and remains prominent upon lowering the intensity scale in Fig. 1d without signs of band folding.

The doping and temperature dependence of the VBG pseudogap is shown in Fig. 2. With increasing doping, the distribution of the valence bond in Fig. 2a sharpens around zero, the VBG order parameter δ_χ reduces, and the Fermi arc length increases in agreement with ARPES experiments. Note that while the density of off-plane dopants increases with doping, δ_χ decreases due to improved screening by more mobile carriers such that the potential V_i has weaker fluctuations. The doping evolution of the IDOS is shown in Fig. 2b. The pseudogap becomes smaller and shallower with increasing doping and becomes undiscernible beyond $x = 0.22$ on the shoulder of the van Hove peak. The extracted pseudogap has a doping dependence that follows $\Delta_{pg} \simeq (J/8) \sqrt{\sum_i (\sum_j g_{ij}^\chi \chi_{ij} d_{ij})^2 / N_s}$, as shown in Fig. 3c. The temperature evolution of the pseudogap obtained by minimizing the free energy of the renormalized mean field theory is shown in Fig. 2c at $x = 0.125$. The onset temperature $T^* \simeq 16\text{meV}$ is clearly seen to be determined by the thermal filling of the VBG pseudogap.

The momentum-dependence of the symmetrized spectral

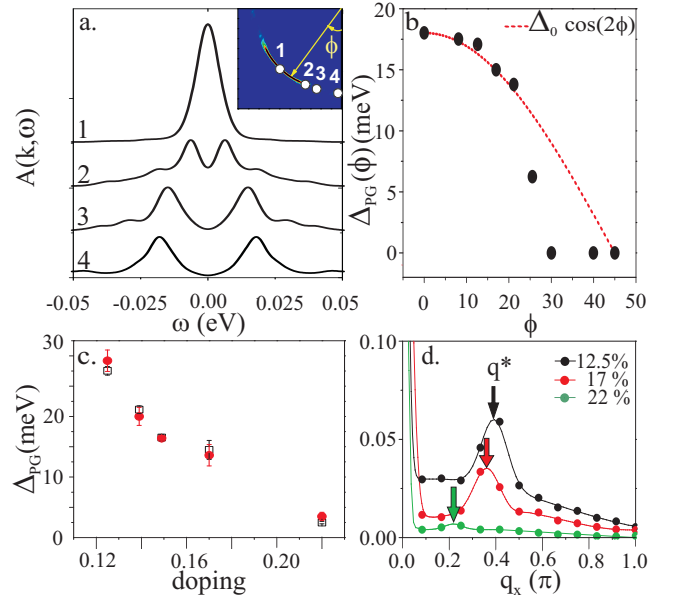


Figure 3: Angular dependence of symmetrized spectral function (a) and the pseudogap (b). (c) Doping dependence of pseudogap from IDOS (circles) and d -wave valence bond order parameter (squares). (d) $|\chi_d(q)|$ along q_x -direction with peaks at q^* marked in Fig. 1d.

function $A(k, \omega)$ is plotted in Fig. 3a at Fermi level for $x = 0.14$. It shows gapless quasiparticle excitations along the arc and the opening of the pseudogap at the arc tip that increases toward the antinodes. The angular dependence of the pseudogap extracted this way is shown in Fig. 3b. Away from the zero-gap Fermi arc regime, the pseudogap follows the d -wave form consistent with the d -wave nature of the VBG. The line-shape in Fig. 3a shows that the pseudogap near the antinodes is a *soft gap*. This important prediction of the VBG is consistent with the ARPES experiments that coined the term “pseudogap” originally [2, 3], and differs from the naive picture of a hard gap that depletes all states near the antinodes below the pseudogap energy scale. These in-gap states contribute to the incoherent spectral weight at low energies and have important consequences in the SC state.

The pseudogap in the VBG theory does not require the antinodal FS sections to be parallel and is not sensitive to the details of the FS. We obtain completely similar results using a different set of hopping parameters $t = (480, -160, 50, 50, -50)\text{meV}$ as in Ref.[23] that does not favor the nesting condition near the antinodes. These will be used later for the SC state. A band dispersion showing flatness near the antinodes as observed experimentally suffices. The propensity toward the VBG is due to an enhanced static susceptibility broadly peaked around the q^* shown in Fig. 1 that enables electronic disorder to pin the VBG with a distribution of $\chi_d(q)$ peaked around q^* . In Fig. 3d, we show the Fourier power spectrum $|\chi_d(q)|$ plotted along the q_x -direction. Both the peak and the incommensurate q^* decrease with increasing doping. At $x = 0.14$, $q^* \simeq (\pm 0.4\pi, 0)$, indicative of glassy $\sim 5 \times 5$ checkerboard patterns for the valence bond.

Superconducting phase. In the SC phase below T_c , the VBG

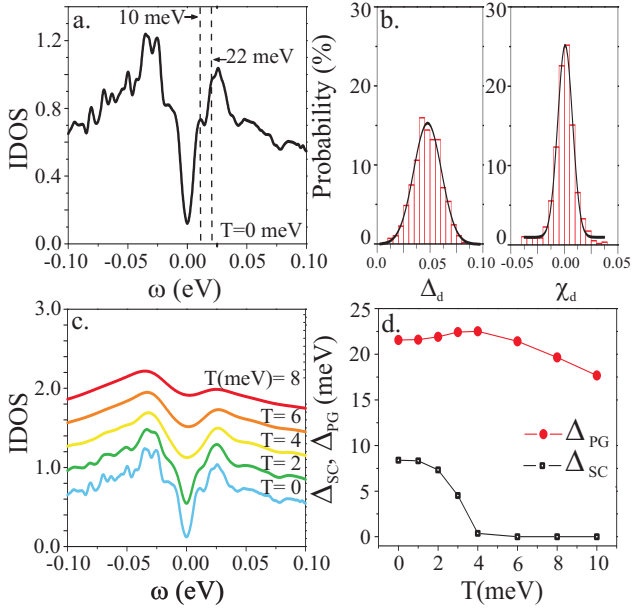


Figure 4: SC state at $x = 0.14$. (a) Averaged DOS showing SC gap and VBG pseudogap. (b) Distributions of χ_d and $\Delta_d = \sum_j d_{ij} \Delta_{ij}/4$. Temperature evolution of IDOS (c) and SC gap and pseudogap (d).

can coexist and compete with an inhomogeneous d -wave superconductor; both originate from the superexchange interaction. Although the Gutzwiller factors $g_{ij}^\chi = g_{ij}^\Delta$, charge fluctuations at finite doping, and in particular, the pair-breaking induced by inter-site Coulomb repulsion will weaken the singlet pairing channel [32]. Moreover, the electron-phonon interactions have been shown to promote the d -wave charge density wave [33, 34]. To incorporate these effects into the renormalized mean field theory in Eq. (2), we use $g_{ij}^\chi = g_{ij}^\Delta$ and $g_{ij}^\Delta = pg_{ij}^\chi$ with $p = 0.475$, which separates the two energy gap scales in the underdoped regime. The IDOS at $T = 0$ is shown in Fig. 4a for $x = 0.14$. It clearly displays two gaps: a smaller SC gap around $\Delta_{SC} \simeq 10$ meV and a large pseudogap $\Delta_{PG} \simeq 22$ meV inherited from the normal state, in agreement with STM experiments on La-Bi2201 [8, 9]. Both gaps are inhomogeneous with order parameter distributions plotted in Fig. 4b. The temperature evolution of the IDOS (Fig. 4c) clearly shows that the SC gap and coherence peaks vanish above $T_c \sim 4$ meV as the system enters the pseudogap phase. Interestingly, as T is increased toward T_c in Fig. 4d, the pairing gap and the pseudogap show opposite temperature dependence, a typical feature of coexisting but competing order.

In Figs. 5a and 5b, the local DOS is shown along two line cuts on a typical sample at $x = 0.14$. The evolution of the line-shape agrees rather well with the STM conductance spectra observed in La-Bi2201 [8, 9], exhibiting two spatially coexisting low energy gaps. The momentum dependence of the two gaps, calculated from the single-particle spectral function $A(k, \omega)$, is plotted along the underlying FS in Fig. 5c. Remarkably, the d -wave pairing gap extends beyond the Fermi arc into the antinodal regime. The coexistence of the two gaps off the Fermi arc in momentum space is an important predic-

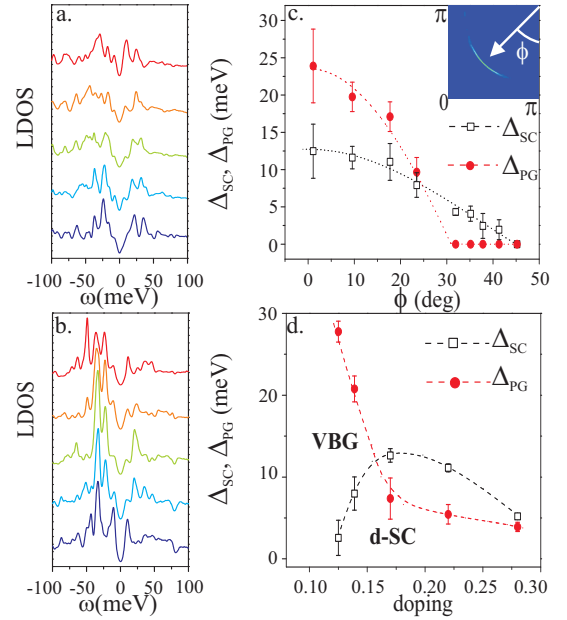


Figure 5: Local DOS along two line cuts (a) and (b) and angular dependence of SC gap and pseudogap at $x = 0.14$. (c). (d) Δ_{SC} and Δ_{PG} as a function of doping.

tion of the present theory. Physically, this is a consequence of the softness of the normal state pseudogap discussed above which allows pairing of the antinodal states inside the pseudogap. The ground state below T_c is thus a coherent mixture of d -wave VBG and SC pairs; there are traits of the glassy valence bond order in the pairing gap near the antinodes and *vice versa*. Although the large incoherent background and the inelastic life-time broadening tend to mask the coherent peak and the pairing gap near the antinode in the spectral function, recent high resolution ARPES experiments performed on La-Bi2201 indeed observe two gaps near the antinodes [9, 35].

In summary, we presented a VBG theory for the essential features of the normal state pseudogap and the two-gap phenomena in the SC state. In Fig. 5d, we construct a theoretical phase diagram using the doping dependence of the d -wave pairing gap and the VBG pseudogap. It captures the basic topology of the global phase diagram of the high- T_c cuprates. Although the present theory does not include a precursor pairing induced pseudogap above T_c , it does not rule out such a possibility due to fluctuations beyond the Gutzwiller theory.

We thank H. Ding, V. Madhavan, S. Zhou, and C. Li for useful discussions. This work was supported in part by DOE grant DE-FG02-99ER45747 and NSF grant DMR-0704545.

-
- [1] For a recent review, see P.A. Lee et al., Rev. Mod. Phys. **78**, 17 (2006).
 - [2] A.G. Loeser et al., Science **273**, 325 (1996).
 - [3] H. Ding et al., Nature **382**, 51 (1996).
 - [4] K. Tanaka et al., Science **314**, 1910 (2006).
 - [5] W.S. Lee et al., Nature, **450**, 81 (2007).

- [6] T. Kondo et al., Phys. Rev. Lett. **98**, 267004 (2007).
- [7] M. Le Tacon et al., Nature Phys. **2**, 537 (2006).
- [8] M. C. Boyer et al., Nature Phys. **3**, 802 (2007); W.D. Wise et al., arXiv:0806.0203.
- [9] J.-H. Ma, et al., arXiv:0807.3294 (2008).
- [10] M.R. Norman, et al., Phys. Rev. **B76**, 174501 (2007), and references therein.
- [11] A. Kanigel et al., Phys. Rev. Lett. **99**, 157001 (2007).
- [12] M. Civelli et al., Phys. Rev. Lett. **100**, 046402 (2008).
- [13] C. Li et al., Phys. Rev. **B73**, 060501 (2006).
- [14] S.H. Pan et al., Nature **413**, 282 (2001).
- [15] C. Howald et al., Phys. Rev. **B64**, 100504 (2001).
- [16] K.M. Lang et al., Nature **415**, 412 (2002).
- [17] K. McElroy et al., Science **309**, 1048 (2005).
- [18] T. Hanaguri et. al. Nature **430**, 1001 (2004).
- [19] M. Vershinin et al., Science **303**, 1995 (2004).
- [20] K. McElroy et al. Phys. Rev. Lett. **94**, 197005 (2005).
- [21] Y. Kohsaka et al., Science **315**, 1380 (2007).
- [22] Z. Wang et. al. Phys. Rev. **B65**, 064509 (2002).
- [23] S. Zhou et al., Phys. Rev. Lett. **98**, 076401 (2007).
- [24] P.W. Anderson, Science **235**, 1196 (1987).
- [25] I. Affleck, *et. al.*, Phys. Rev. **B38**, 745 (1988).
- [26] D. Rokhsar and S.A. Kivelson, Phys. Rev. Lett. **61**, 2376 (1988).
- [27] P.W. Anderson et al., J. Phys. Cond. Matt. **16** R755 (2004).
- [28] S.A. Kivelson et al., Rev. Mod. Phys. **75**, 1201 (2003).
- [29] M.R. Norman and H. Ding, Phys. Rev. **B57**, 11089 (1998).
- [30] D. Vollhardt, Rev. Mod. Phys. **56**, 99 (1984).
- [31] F.C. Zhang, et al., Supercond. Sci. Technol. **1**, 36 (1988).
- [32] S. Zhou and Z. Wang, Phys. Rev. **B70**, 020501 (2004).
- [33] D.M. Newns and C.C. Tsuei, Nature Phys. **3**, 184 (2007).
- [34] J.-X. Li et al., Phys. Rev. **B74**, 184515 (2006).
- [35] J. Wei et al., arXiv:0801.2212 (2008).